Fabrication of Polyphosphazene Covalent Triazine Polymer with Excellent Flame Retardancy and Smoke Suppression for Epoxy Resin

Yunzhi Fang, Junshuai Miao, Xingwen Yang, Yun Zhu, Guiyou Wang

PII: S1385-8947(19)33245-0
DOI: https://doi.org/10.1016/j.cej.2019.123830
Reference: CEJ 123830

To appear in: *Chemical Engineering Journal*

Received Date: 17 September 2019
Revised Date: 11 December 2019
Accepted Date: 14 December 2019

Please cite this article as: Y. Fang, J. Miao, X. Yang, Y. Zhu, G. Wang, Fabrication of Polyphosphazene Covalent Triazine Polymer with Excellent Flame Retardancy and Smoke Suppression for Epoxy Resin, *Chemical Engineering Journal* (2019), doi: https://doi.org/10.1016/j.cej.2019.123830

Fabrication of Polyphosphazene Covalent Triazine Polymer with Excellent Flame Retardancy and Smoke Suppression for Epoxy Resin

Yunzhi Fang, Junshuai Miao, Xingwen Yang, Yun Zhu, Guiyou Wang*

Shanghai Key Laboratory of Advanced Polymeric Materials, School of Materials Science and Engineering, East China University of Science and Technology, Shanghai 200237, China

* Corresponding to: Guiyou Wang, Email address: guiyouwang@ecust.edu.cn

GRAPHICAL ABSTRACT

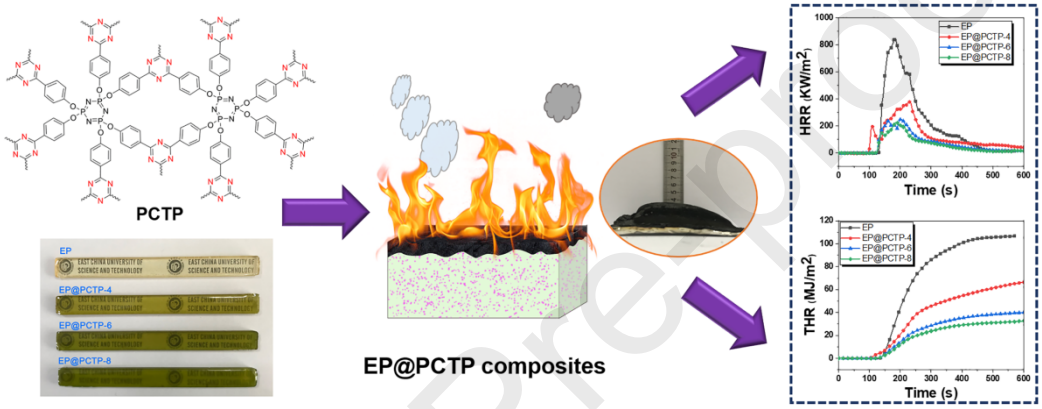

ABSTRACT

A kind of polyphosphazene covalent triazine polymer (PCTP) was fabricated through a facile trimerization reaction of 4-hydroxybenzonitrile substituted hexachlorocyclotriphosphazene (HCCP). The as-prepared PCTP containing phosphorus and nitrogen elements was added into epoxy resins (EP) to improve their fire resistance and smoke suppression property. As obtained from cone calorimeter test, compared with the neat EP, the values of peak heat release rate (P-HRR), total heat release (THR) and total smoke production (TSP) of EP@PCTP composites were reduced by 73%, 69% and 42%, respectively, when 8.7 phr PCTP was loaded into the EP matrix. Meanwhile, the limiting oxygen index (LOI) value was also increased greatly from 22.3% to 28.0%, and the EP composites successfully passed UL-94 V-0 rating with 6.4 phr PCTP incorporated. The results may be resulted from the more compact and higher coherence char layer of EP@PCTP composites, and PCTP could function both in condensed and gaseous phases due to the barrier effect and dilution effect during the combustion. The water resistance of the EP matrix

was also enhanced effectively due to the presence of PCTP. In addition, the nearly unchanged glass transition temperature (T_g) and mechanical properties of the resultant EP@PCTP composites confirmed the excellent compatibility between PCTP and EP matrix, which endows its promising application potential in polymer materials.

Keywords: Covalent triazine polymer; Phosphazene derivative; Epoxy resin; Fire safety; Smoke suppression

1. Introduction

Epoxy resins (EP), a type of prominent thermosetting materials, have been widely used in the field of adhesives, paints, laminates and structural composites, etc., owing to their excellent properties such as superior chemical resistance, dimensional stability and outstanding mechanical performance [1-3]. Unfortunately, like many other organic materials, the poor flame resistance of EP extremely restricted their further applications in electrical and electronic industries [4-6]. What's more, the large amounts of dense smoke as well as toxic gases such as CO and NO generated during the combustion could cause huge damages both to human lives and their properties, and could also have a serious impact on social and economic development [7, 8].

Over the past decades, extensive efforts have been devoted to reduce the fire hazard of EP. Halogenated flame retardants (FRs), an efficient strategy in the past, however, have been prohibited in many countries due to their potential hazards to human health and environment [9]. Alternatively, phosphorus-containing FRs are efficient in improving the fire safety of substrate materials. The blocking and quenching effects of phosphorus and its free radicals contribute to the enhanced flame retardancy and less smoke of the matrix. However, some flame retardant EPs suffer from high water absorption due to the hydrophilicity of certain phosphorus-containing FRs [10-13], which will deteriorate the electronic performance. Nitrogen-based FRs are also candidates for some polymers due to their dilution effect caused by the ignitable gases generated like N_2, NH_3 and NO_2 [14-17]. Nevertheless, many researches have suggested that there exists a favorable synergistic effect between phosphorus and nitrogen elements [18-20]. For example, Gaan et al. investigated the influence of nitrogen-containing additives on the flame retardancy of cotton cellulose, and the results showed that compared with the cotton samples only containing phosphorus element, those having both phosphorus and nitrogen elements achieved higher LOI values and char yields [21]. Duan et al. prepared a phosphorus/nitrogen containing polycarboxylic acid (TMD), and the investigations revealed that TMD exerted bi-phase flame-retardant effects on EP [22]. Hu et al. designed a hyper-branched phosphorus/nitrogen-containing FR (HPNFR) via the transesterification reaction, and it was found that the EP had higher LOI and passed UL-94 V-0 rating [23]. However, these FRs failed to improve the thermal stability of EP, and their impacts on the water resistance were not studied.

Hexachlorocyclotriphosphazene (HCCP), a class of representative organic-inorganic hybrid material with alternating arrangement of phosphorus and nitrogen elements in the backbone, has aroused great concern due to its tremendous thermal stability and outstanding structural flexibility. Due to the presence of active P–Cl bonds, a battery of phosphazene derivatives can be prepared through the reaction of HCCP with amines, phenols, alcohols or thiol compounds [24-26]. The prepared derivatives could be small molecules, as well as branched and crosslinked polymers, which have been applied in the fields of biomaterials, liquid crystals, catalysts, and chemical sensors etc. [27-31]. Until now, many additive and reactive FRs have been prepared from HCCP, among which the compounds with nitrogen-containing heterocycle such as maleimide, triazole and triazine have drawn much attention due to their synergistic effect in improving the fire safety of polymer materials. For instance, Yang et al. reported a phosphazene derivative from HCCP and maleimide, the compound showed flame retardancy both in condensed and gaseous phases [32]. Chen et al. prepared a series of phosphazene-triazine bi-group FRs from HCCP, amine compounds and cyanuric chloride, which could effectively improve the fire resistance of polylactic acid when they were blended with ammonium polyphosphate (APP) [33]. Wen et al. synthesized a cyclotriphosphazene-based chemical from HCCP and piperazine, the chemical exhibited an excellent char-forming property to polypropylene when it was used in combination with 10.0-22.5 wt% microencapsulated APP [34]. Nevertheless, most of them were small molecules or required a complex synthetic procedure. What's more, they exhibited high flame retardancy only when mixed with other additives, thus restricting their practical applications.

Covalent triazine polymers (CTPs) are a subclass of covalent organic frameworks (COFs). The presence of well-defined heteroatoms in the triazine frameworks provides their potential applications in gas adsorption, catalysis and organic dyes etc. [35-37]. However, in spite the fact that CTPs are rich in nitrogen element, the application of CTPs as FRs has been rarely carried out previously. On the other hand, in view of the knowledge that CTPs can be easily prepared through the trimerization reaction of cheap aromatic nitriles with strong Brønsted acids or $ZnCl_2$ as the catalyst, and the P–Cl bonds in HCCP can be replaced by the hydroxyls of 4-hydroxybenzonitrile to obtain a phosphazene monomer containing aromatic nitriles. Thus, a novel CTP with phosphazene structure can be formed through the trimerization of 4-hydroxybenzonitrile

substituted HCCP. The hyper-crosslinked structure as well as the triazine units would exhibit better water-resistance and higher thermal stability [34, 38]. To the best of our knowledge, the preparation of such a CTP with phosphazene units embedded and its application in reducing the fire hazard of EP have not been reported yet.

Herein, we introduce a novel phosphazene-based CTP (PCTP) through the facile trimerization reaction of hexakis-(4-cyanophenyloxy)cyclotriphosphazenes (HCPCP). The designed PCTP was prepared under mild condition, and achieved a high yield (94%) without using triazine-based monomers like melamine, cyanuric chloride and cyanuric acid as the synthesis of most triazine-containing FRs did, which possess the potential for industrial production. The as-synthesized PCTP has both triazine and cyclotriphosphazene units as well as the hyper-crosslinked structure, which might endow it with higher thermal stability, excellent char forming ability and better water resistance than the other micro-molecular cyclotriphosphazene- and triazine-based FRs [39, 40]. PCTP was further applied to improve the fire safety of EP. The morphology, mechanical properties, thermal stability, water absorption, combustion behavior and smoke suppression properties of EP@PCTP composites were investigated. In addition, the possible flame-retardant mechanism of PCTP to reduce the fire risk of EP was also discussed.

2. Experimental section

2.1. Materials

HCCP, anhydrous potassium carbonate (K_2CO_3), 4-hydroxybenzonitrile, trifluoromethanesulfonic acid (CF_3SO_3H), 4, 4'-diaminodiphenylmethane (DDM), chloroform and acetone were purchased from Aldrich Chemical Co., Ltd (Shanghai, China). Diglycidyl ether of bisphenol A (DGEBA) with the epoxy value of 0.51 mol/100 g was supplied by Jiangyin Wanqian Chemical Industry Co. Ltd (Jiangsu, China). Before use, K_2CO_3 was dried at 140 °C for 2 h; acetone and chloroform were dried with $CaSO_4$ and were redistilled. Other reagents were used as received.

2.2. Synthesis of HCPCP

HCPCP was synthesized as follows [41]. HCCP (19.97 g, 57.44 mmol), 4-hydroxybenzonitrile (41.07 g, 344.8 mmol), K_2CO_3 (114.44 g, 828 mmol) and 800 mL acetone were added to a flask. The mixture was then heated to 55 °C and stirred for 10 h under nitrogen

atmosphere. After that, the mixture was concentrated by rotary evaporation and subsequently washed with plenty of distilled water to remove the white salt. The obtained crude product was recrystallized twice in 400 mL DMF, and then dried at 80 °C under vacuum for 24 h to get a white product with a yield of 86% (**Scheme 1**).

2.3. Synthesis of PCTP

PCTP was prepared through one-pot superacid catalytic trimerization reaction of HCPCP in chloroform. In a typical procedure, HCPCP (15.6 g, 18.5 mmol) and 700 mL chloroform were charged into a pre-dried 2-neck round bottom flask under argon atmosphere. The mixture was cooled to 0 °C and CF_3SO_3H (18 g, 120 mmol) was then added dropwise over 30 min. The reaction was continued for 2 h at 0 °C and then maintained for another 22 h at room temperature. The hard, yellow precipitate appeared during the reaction process. After that, an NH_3/H_2O solution (0.5 mol/L) was added and stirred for another 2 h until the mixture became neutral. Finally, the mixture was filtered and washed with distilled water, ethanol and THF successively, and then dried under vacuum for 24 h to obtain a yellow powder with a yield of 94% (**Scheme 1**).

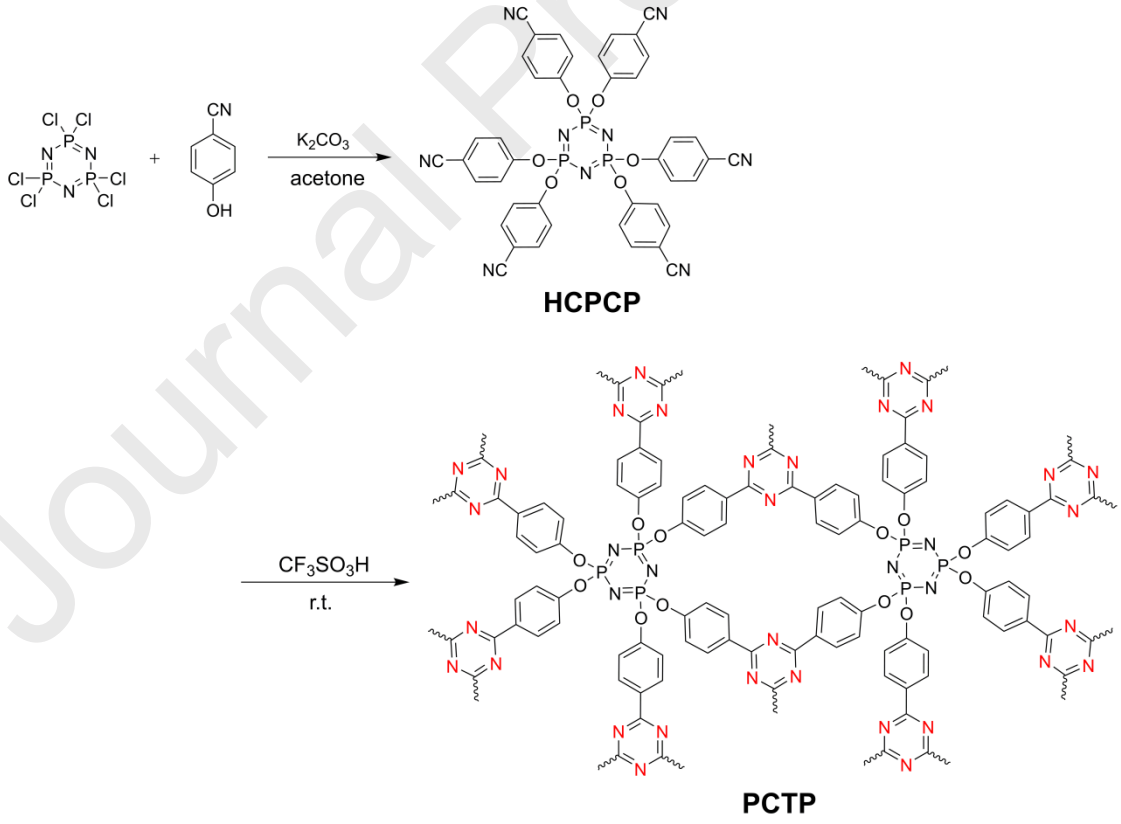

Scheme 1. Synthetic routines of HCPCP and PCTP.

2.4. Preparation of EP@PCTP composites

Firstly, calculated amounts of finely grinded PCTP was dispersed in 100 mL THF, then 100 g DGEBA was added and stirred at 60 °C for 3 h with the aid of ultrasonication. Subsequently, the THF was removed completely under vacuum at 60 °C. After that, 25.74 g DDM melted at 105 °C was added into the mixture and stirred at 220 rpm for 1 ~ 2 min. Then, the mixture was poured into a preheated mold immediately after degassed for another 5 min to remove air bubbles. Finally, the blend was cured at 100 °C for 2 h and 150 °C for 2 h respectively to get EP@PCTP composite samples with different PCTP contents. The formulations of the EP@PCTP composites are listed in **Table 1.**

Table 1 Formulations of EP and EP@PCTP composites.

Sample	DGEBA	DDM	PCTP	PCTP content	
	(g)	(g)	(g)	phr	wt%
EP	100	25.74	0	0	0
EP@PCTP-4	100	25.74	5.24	4.2	4
EP@PCTP-6	100	25.74	8.03	6.4	6
EP@PCTP-8	100	25.74	10.93	8.7	8

2.5. Measurements

Fourier transform infrared (FTIR) spectra of all samples were recorded on a Nicolet 5700 IR spectrometer in the range of 4000 ~ 400 cm^{-1} with a resolution of 4 cm^{-1}. The samples were grinded with KBr and pressed into pellets before characterization.

^{1}H NMR spectrum of HCPCP was obtained at room temperature on a Bruker AVANCE 400 MHz spectrometer. Dimethyl sulfoxide-d_6 (DMSO-d_6) was used as solvent.

The solid-state ^{31}P CP/MAS NMR spectrum was obtained using an AVANCEIII 500 MHZ super conducting Fourier NMR spectrometer.

Electrospray ionization mass spectrometry (ESI-MS) of HCPCP was performed by using a XEVO G2 TOF apparatus.

X-Ray photoelectron spectroscopy (XPS) measurement was conducted on a Thermo ESCALAB 250XI spectrometer to obtain the relative elemental compositions and the valence states of PCTP.

Energy-dispersive X-ray spectroscopy (EDS) was performed by using a QUANTAX 400-30 apparatus.

Differential scanning calorimetry (DSC) were achieved on a DSC Q2000 (TA Instruments) to

obtain the glass transition temperatures (T_g) of EP and its composites. All the measurements were performed under N_2 atmosphere with a heating rate of 10 °C·min^{-1} from room temperature to 200 °C.

Thermo-gravimetric analysis (TGA) of samples was monitored by using the NETZSCH STA409PC/4/H TGA thermal analyzer. Each sample (8 ~ 10 mg) was placed in a platinum pan and heated from room temperature to 800 °C at a heating rate of 10 °C·min^{-1} under the N_2 or air atmosphere with a flow rate of 20 mL·min^{-1}.

The limiting oxygen index (LOI) values were measured on a JF-3 oxygen index instrument according to ASTM D2863-06, with the specimen size of 130 × 6.5 × 4 mm^3. The vertical burning (UL-94) were conducted on a FTT0082 instrument according to ATSM D3801, with the specimen size of 130 × 13 × 3.2 mm^3.

The water resistance of EP@PCTP composites was measured according to the following process. The samples were soaked in distilled water at 70 °C, and the water was refreshed every 24 h. After certain periods, the samples subjected to tests were taken out and the water on the surface of samples was wiped carefully. The water absorption percentage (WAP) of the samples was calculated using the following equation:

$$WAP = [(W_1-W_0) / W_0] \times 100\% \quad (1)$$

Where W_0 represents the initial mass, and W_1 is the mass of treated samples after immersed in water for different periods of time.

The combustion behaviors of EP and EP@PCTP composites were evaluated on a FTT cone calorimeter at a heat flux of 35 kW·m^{-2}, which corresponds to a mild fire scenario. The size of the specimens was 100 × 100 × 4 mm^3 and each specimen was mounted on aluminum foil during the test.

Morphological studies of char residues and fracture surface of EP and EP@PCTP composites were carried out using an S-3400N scanning electron microscope (SEM) at an acceleration voltage of 15 kV.

Thermogravimetric analysis/Fourier transform infrared spectrometry (TG-FTIR) was characterized by utilizing a NETZSCH TG 209F3 thermal analyzer connected with a Nicolet 6700 IR spectrometer. The sample (around 8 mg) was heated from 35 to 800 °C at 10 °C·min^{-1} under

N_2 atmosphere.

Laser Raman spectroscopy (LRS) measurements were conducted on an INVIA reflex Laser Micro-Raman Spectrometer at room temperature with a 514.5 nm argon laser line.

Tensile and flexural tests were performed on a SANS tester at room temperature according to ASTM D638-2010 and ASTM D790-2003, respectively. The size of dump-bell shaped tensile samples was 115 × 20 × 4 mm^3, and the size of bending samples was 80 × 10 × 4 mm^3. The values of both tests reflected an average of five tests.

3. Results and discussion

3.1 Characterization of HCPCP

The structure of HCPCP was characterized by FTIR, ^{1}H NMR and ESI. In the FTIR spectrum of HCPCP (**Fig. 1a**), typical peaks at 1201 and 846 cm^{-1} were attributed to P=N and P–N stretching vibration of the phosphazene groups, respectively [42, 43]. The distinct absorption of P–O–C_{Ar} band can be observed at 1017 and 944 cm^{-1}. Compared with FTIR spectrum of HCCP, the appearance of a new sharp absorption band of C≡N at 2232 cm^{-1} and the disappearance of P–Cl band at 600 and 519 cm^{-1} confirmed the reaction between HCCP and 4-hydroxybenzonitrile. In the ^{1}H NMR spectrum (**Fig. 1b**), the signals at 7.18 and 7.84 ppm were assigned to the protons in the benzene rings of aromatic nitriles, and the integrated area ratio of the two peaks was close to 1:1. No extra signals arising from impurity were detected, indicating that the structure of HCPCP was consistent with our expectation. In addition, ESI-MS result in **Fig. S1** showed that the measured m/z of HCPCP (866.0961 $[M + Na]^+$) was very close to the calculated value (866.0960 $[M + Na]^+$), which further proved that HCPCP was synthesized successfully.

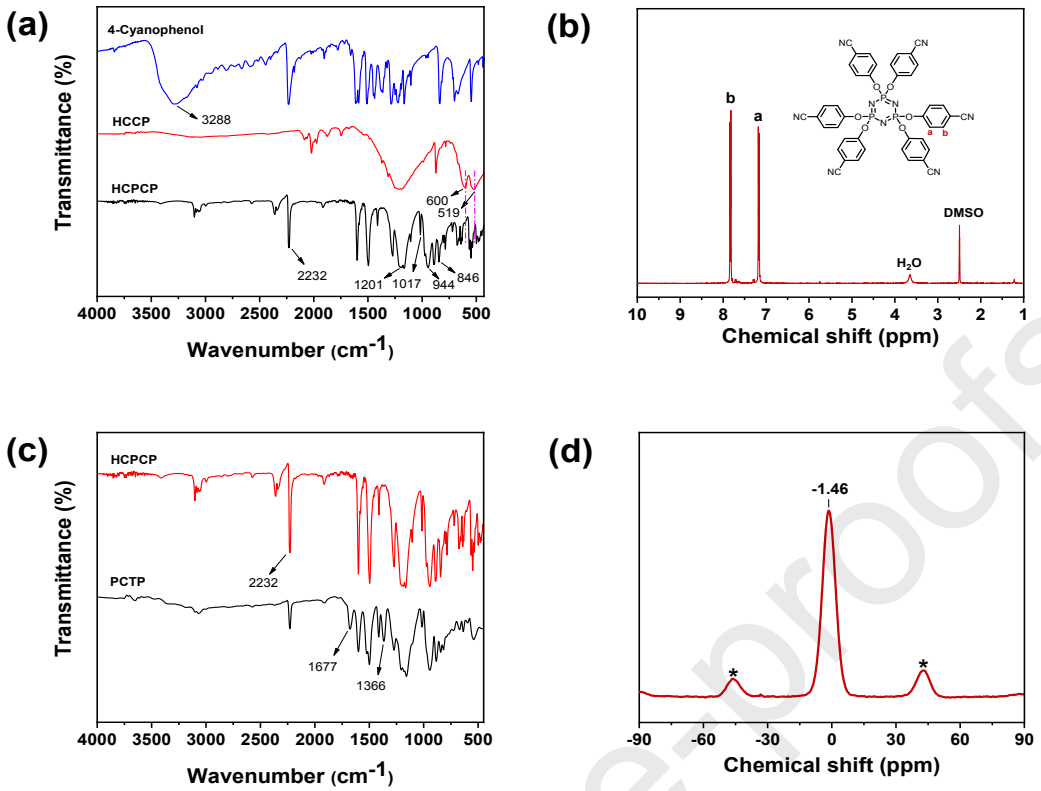

Fig. 1. FTIR spectra of (a) HCPCP and (c) PCTP; (b) ^{1}H NMR spectrum of HCPCP and (d) ^{31}P NMR spectrum of PCTP.

3.2 Characterization of PCTP

As illustrated in **Fig. 1c**, compared with the FTIR spectrum of HCPCP, the two new strong bands appeared at 1677 and 1366 cm^{-1} proved the generation of triazine rings [44, 45]. Meanwhile, the intensity of carbonitrile band at around 2232 cm^{-1} in the PCTP sample was decreased significantly, which indicated that there only existed a few terminal nitrile moieties in PCTP. In addition, the solid-state ^{31}P CP/MAS NMR spectrum of PCTP (**Fig. 1d)** exhibited only one resonance signal at -1.46 ppm, which implied that all the P atoms in PCTP were under a magnetically equivalent environment [46, 47].

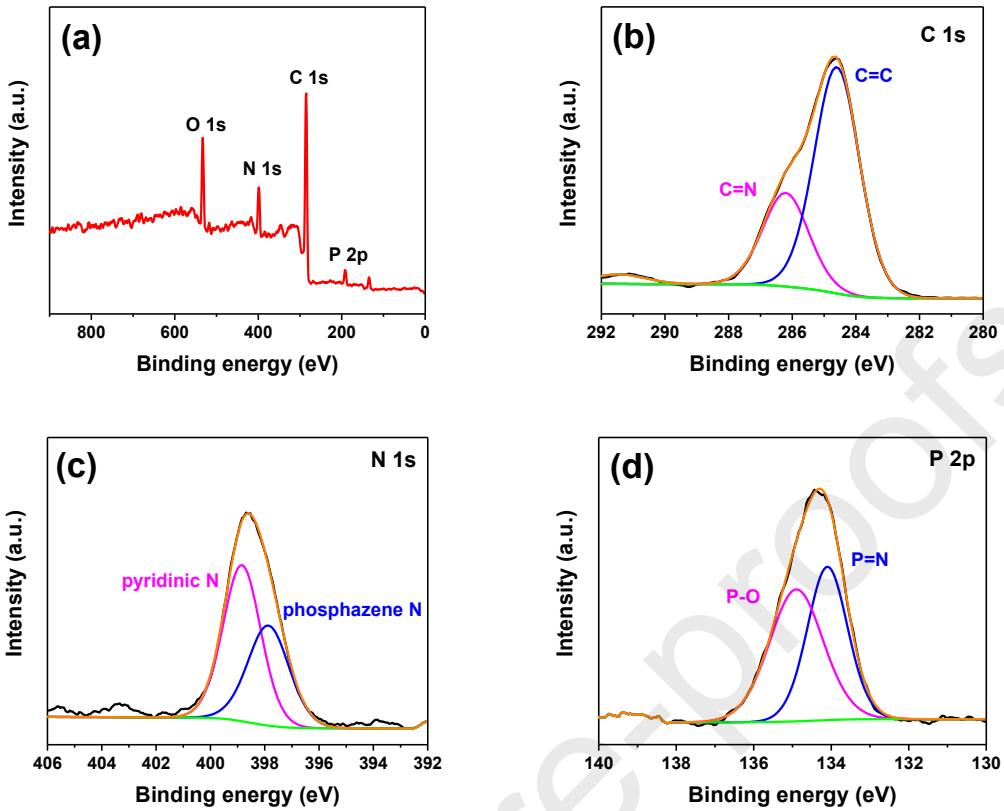

Fig. 2. (a) XPS survey spectrum of PCTP; high-resolution XPS spectra of PCTP in the (b) C 1s, (c) N 1s, and (d) P 2p regions.

According to the XPS survey spectrum in **Fig. 2a**, the atomic percentage of C, N, O and P was 69.16%, 12.11%, 14.40% and 4.33%, respectively, which nearly matched the calculated values (C:70%, N:15%, O:10%, P:5%). **Fig. 2b-d** portrayed the high-resolution scans of the C 1s, N 1s, and P 2p. The C 1s signal of the PCTP exhibited two main peaks with binding energies at 286.3 and 284.6 eV, which were attributed to C=N and C=C bonds, respectively [48]. In the N 1s spectrum, two binding states could be separated, one at 398.8 eV was derived from the pyridinic nitrogen (C=N–C) in the triazine units of PCTP, and the other at 397.9 eV could be ascribed to the nitrogen in phosphazene [49-51]. In addition, the P 2p spectrum indicated the co-existence of the P-O (134.9 eV) and the P=N bonds (134.1 eV) in the structure [52, 53]. The above analysis confirmed that the structure of PCTP was identical with the expected design.

EDS analysis was further conducted to verify the elemental compositions of PCTP. It is observed from the EDS-mapping images in **Fig. 3** that C, O, N, and P elements existed in the

sample and all of the elements in PCTP dispersed uniformly in the skeleton of polymers, which further corroborated the successful preparation of PCTP.

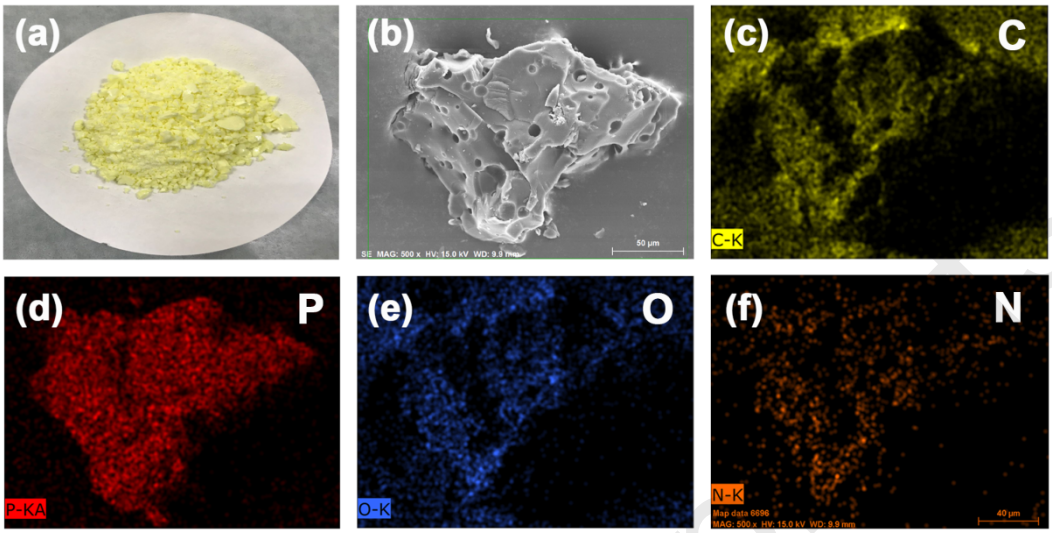

Fig. 3. (a) Digital photograph of bulk PCTP; (b) SEM image, and (c-f) EDS-mapping images of PCTP.

PCTP was not dissolved in any common solvents such as THF, acetone, DMF, and DMSO, etc. Its thermal stability was characterized by TGA (**Fig. S2**). The 10 wt% loss temperature ($T_{10\%}$) of PCTP was 429 °C, and the char yield at 800 °C (R_{800}) reached up to 67 wt%, which indicated its high thermal stability and good charring property. Such pretty properties came from the thermally stable cyclotriphosphazene and triazine groups, and the hyper-crosslinked structure of PCTP. In the DTG curve (**Fig. S2**), a three-step decomposition process of PCTP can be observed, which could be ascribed to the weight loss of small amount of residual water in post-treatment process, the breakdown of skeleton and decomposition of char residues, respectively.

3.3 Thermal properties of EP@PCTP composites

T_g is generally considered to be a significant parameter in evaluating the thermal and compatibility properties of polymeric materials. **Fig. 4a** shows that the EP@PCTP composite samples presented a slightly higher T_g than that of pure EP sample, indicating the increase of rigidity and the favorable compatibility between EP matrix and PCTP particles. The results may be caused by two factors. On the one hand, the rigid nature of PCTP may confine the mobility of EP chains to some extent; on the other hand, the residual terminal nitrile groups in the PCTP may

react with the epoxide groups during the curing process and thus increase the compatibility and crosslink density of composites [54]. Interestingly, the EP@PCTP composites displayed a good transparency (**Fig. 4b**), which suggests their potential applications in some fields such as LED packaging materials [19].

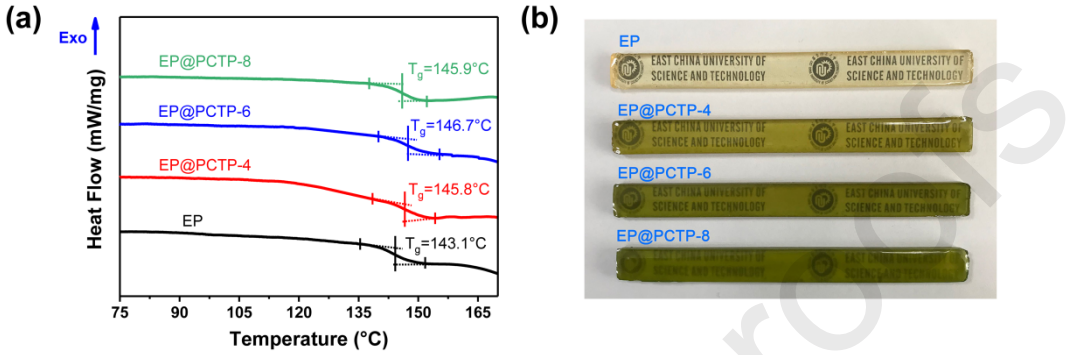

Fig. 4. (a) DSC curves of EP and EP@PCTP composites; (b) digital photographs of EP and EP@PCTP composite samples.

In order to investigate the influence of PCTP on the thermal degradation properties of EP matrix, the thermal stability of EP@PCTP composites in nitrogen and air atmospheres was evaluated (**Fig. 5**), and the detailed data such as $T_{10\%}$, the temperature at maximum weight loss rate (T_{max}) and R_{800} are summarized in **Table S1**. **Fig. 5a** shows that in nitrogen atmosphere, EP and EP@PCTP composites displayed only one decomposition process. $T_{10\%}$ and T_{max} of all the composites were lower than those of pure EP, and they decreased with the increase of PCTP content. This may be attributed to the breakdown of unstable P–O–C bonds existed in the PCTP [55, 56]. However, EP@PCTP composites exhibited a higher R_{800} value than pure EP. For instance, the R_{800} of EP@ PCTP-8 (24.9 wt%) was much higher than that of neat EP (17.9 wt%). This result implied that PCTP could promote the formation of compact char layer, and the phosphorus-rich char layer could play as an effective shield to delay and prohibit the heat and mass transfer, hence, the thermal resistance of EP matrix was improved [57].

In air atmosphere (**Fig. 5c**), the thermal degradation behavior of EP@PCTP composites was mainly divided into two stages. The decomposition trend of the former stage was similar to those in nitrogen atmosphere, while the second stage took place at 470-650 °C was ascribed to the thermal oxidation degradation of the unstable char residues formed in the former stage. In DTG curves (**Fig. 5d**), the changing trend of T_{max2} was not obvious with the increasing content of PCTP,

which may be due to the fact that T_{max2} was mainly determined by the EP matrix itself. The T_{max2} values for EP@PCTP composites were a bit higher than that of the pure EP, demonstrating that EP@PCTP composites were more stable in high temperature region. Furthermore, the improvement of T_{max2} was more obvious than other reported FRs employed in EP [58-60], suggesting that PCTP has a more positive impact on the thermal stability of EP under air atmosphere. In addition, the R_{800} of pure EP was only 0.33 wt%, while those of EP@PCTP composites improved significantly from 0.33 wt% to 2.14 wt% with the increase of PCTP. Such properties would greatly benefit the flame retardancy of EP matrix.

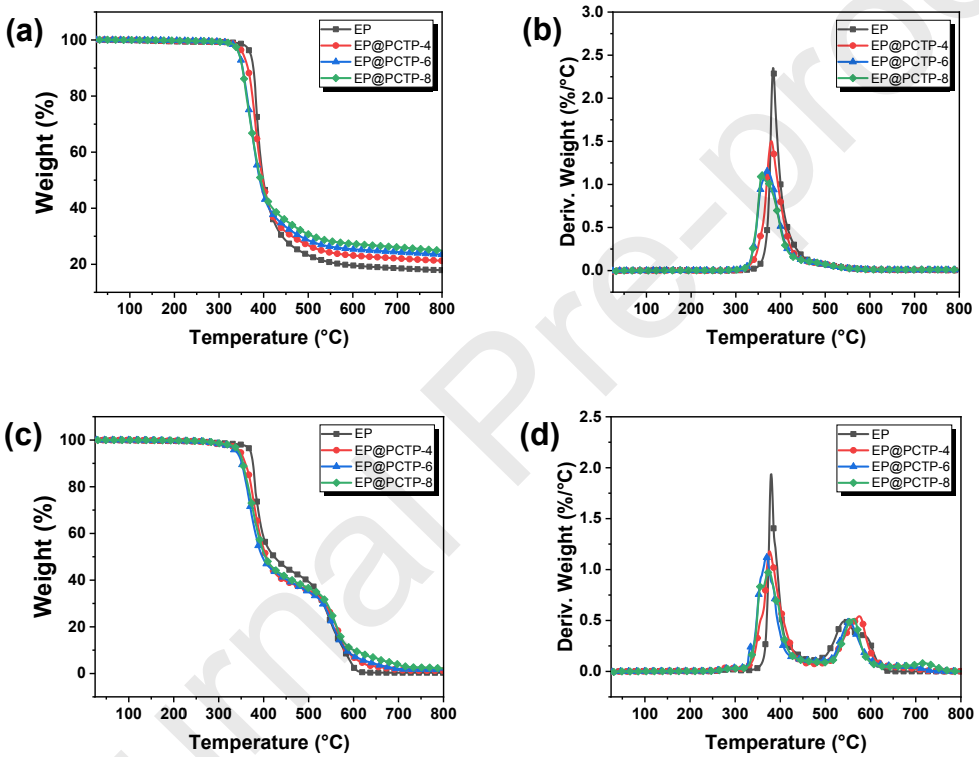

Fig. 5. TGA and DTG curves of EP and EP@PCTP composites in nitrogen (a, b) and air (c, d) atmospheres.

3.4 Combustion behaviors of EP@PCTP composites

The flame retardancy of PCTP was firstly evaluated by LOI and UL-94 tests. As shown in **Table 2**, the LOI values increased dramatically from 22.3% to 28.0% when the PCTP content was increased from 0 to 8.7 phr. As for UL-94 test, the pure EP achieved a longer burning time and received no rating. However, the UL-94 rating of EP composites was promoted with the addition of PCTP and passed the UL-94 V-0 rating when the PCTP content was 6.4 or 8.7 phr. The results

indicated that the incorporation of PCTP could greatly enhance the flame resistance of the EP matrix.

Table 2 LOI and UL-94 results of EP and EP@PCTP composites.

Sample	LOI (%)	UL-94		
		t_1/t_2 (s)[a]	Dripping	Rating
EP	22.3	86.2/7.7	No	No rating
EP@PCTP-4	23.8	17.8/3.3	No	V-1
EP@PCTP-6	26.5	5.3/2.5	No	V-0
EP@PCTP-8	28.0	3.2/2.4	No	V-0

[a] Average burning time after the 10 s ignition.

Cone calorimetry is another significant technique in bench scale to quantitatively assess the fire properties of materials, in which some critical parameters are closely related to the real combustion behaviors. **Fig. 6a-d** display the heat release rate (HRR), total heat release (THR), smoke release rate (SPR), and total smoke production (TSP) curves of prepared composites, and the specific values are listed in **Table 3**. **Table 3** shows that the time to ignition (TTI) of EP@PCTP-4 was much lower than that of pure EP, while the TTI values increased appreciably when the PCTP content further moved to 6.4 and 8.7 phr. It was possible that the lower TTI value of EP@PCTP-4 came from the lower $T_{10\%}$ value compared with the pure EP. However, when the loading of PCTP reached up to a higher proportion, enough nonflammable gases produced could in turn to dilute the ignitable gases, which could cause a higher TTI value [61, 62].

Fig. 6a and **6b** show that pure EP burned dramatically after ignition with a peak HRR (P-HRR) value of 847.6 $kW \cdot m^{-2}$ and a THR value of 106.7 $MJ \cdot m^{-2}$, while the corresponding values changed largely with the incorporation of PCTP. The P-HRR and THR dropped sharply by 55% and 32%, respectively, with only 4.2 phr loading of PCTP in the EP matrix. Furthermore, the 8.7 phr loading of PCTP in the EP brought about a maximum 73% and a maximum 69% diminutions in P-HRR and THR, respectively, demonstrating the superior fire hazard resistance of PCTP to the EP matrix. In order to compare the efficiency of flame retardancy of PCTP, **Table 4** summarizes the cone calorimeter data of several phosphorus/nitrogen-based FRs applied in the EP. Obviously, PCTP exhibited superb flame retardancy in comparison to other FRs.

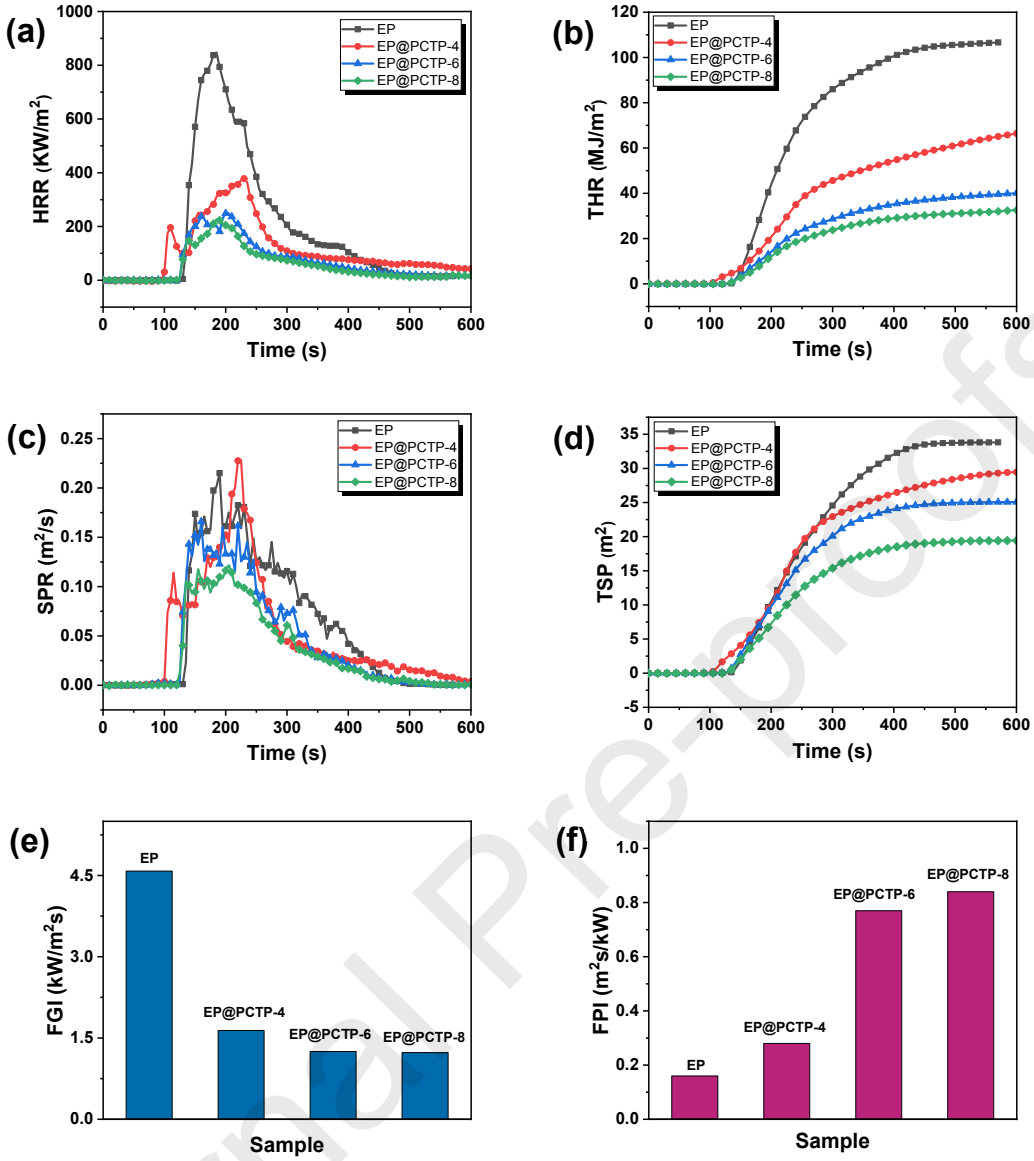

Fig. 6. (a) HRR, (b) THR, (c) SPR, (d) TSP, (e) FGI and (f) FPI results of EP and EP@PCTP composites.

Table 3 Cone calorimeter data of EP and EP@PCTP composites.

Sample	TTI (s)	P-HRR ($kW \cdot m^{-2}$)	THR ($MJ \cdot m^{-2}$)	TSP (m^2)	av-CO ($kg \cdot kg^{-1}$)	av-CO_2 ($kg \cdot kg^{-1}$)	Residue (wt%)
EP	136	847.6	106.7	33.7	0.0498	1.0763	10.8
EP@PCTP-4	106	378.1	72.9	29.5	0.0602	1.0557	22.7
EP@PCTP-6	191	249.3	40.3	25.1	0.0443	0.7022	25.2
EP@PCTP-8	192	227.1	33.3	19.4	0.0409	0.6135	28.5

It is well known that the most casualties in a fire accident are always caused by the smoke and toxic gases released in a burning building. Hence, the smoke emission behavior of a material must be taken into serious consideration. The SPR and TSP curves (**Fig. 6c** and **6d**) show that the SPR and TSP values of pure EP are much higher than those of EP@PCTP composites. The TSP values of EP@PCTP composites reduced appreciably from 33.7 to 19.4 m^2 with the increase of PCTP content, indicating the excellent smoke suppression property of PCTP to the EP matrix. The results could be ascribed to the catalytic charring effect of PCTP, which delayed the diffusion of pyrolysis components and protected the unburned substances inside from exposing to the fire [63]. Moreover, the emissions of CO and CO_2 (**Fig. S3a** and **S3b)** were significantly suppressed with the incorporation of PCTP, which further confirmed the excellent performance of PCTP on harmful gases suppression.

Table 4 Cone calorimeter data of different FRs for EP matrix.

FRs	FR content (phr)	The decrease rate (%)			Heat flux ($kW \cdot m^{-2}$)	Reference
		P-HRR ($kW \cdot m^{-2}$)	THR ($MJ \cdot m^{-2}$)	TSP (m^2)		
BPFA	9.9	47	29	48	50	[51]
HAP-DOPO	10.3	57	/	/	50	[64]
BPA-BPP	9.9	60	11	31	35	[65]
BPS-BPP	9.9	46	15	71	35	[66]
PCTP	8.7	73	69	42	35	This work

Fire growth index (FGI) and fire performance index (FPI) are two important derivative parameters from cone calorimeter test in order to evaluate the flame retardancy of materials. FGI was defined as the proportion of P-HRR and time to P-HRR (t-PHRR), the higher the value, the faster the fire spreads [67, 68]. As shown in **Fig. 6e**, the FGI values of EP@PCTP composites were much lower than that of pure EP. FPI was calculated from the proportion of TTI and P-HRR, which correlated well with the result of large-scale experiments in the case of fire safety. FPI is in negative correlation to the fire hazard, the lower the value of FPI, the quicker the flashover starts [20]. As depicted in **Fig. 6f**, it was obviously that FPI improved with the increase of PCTP, which further corroborated the remarkable property of PCTP in reducing the fire risk of EP matrix.

3.5 Flame retardant mechanism

3.5.1 Morphology and structure of char residues

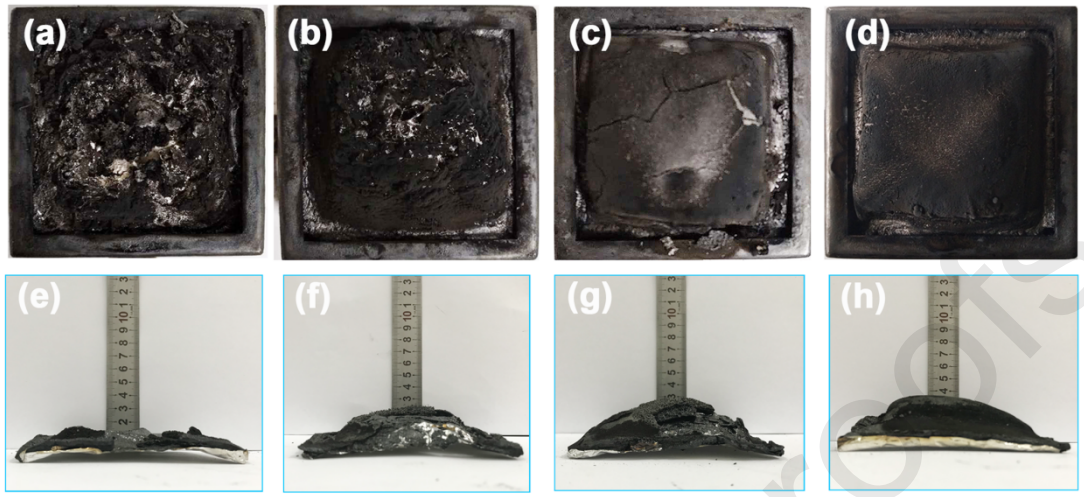

Fig. 7. Digital photographs of the char residues from top view and side view for (a, e) EP, (b, f) EP@PCTP-4, (c, g) EP@PCTP-6 and (d, h) EP@PCTP-8 after cone calorimeter test.

The char residues of polymer materials after combustion could provide some significant information about the flame retardant mechanism. **Fig. 7** exhibits the char residue images of EP and EP@PCTP composites captured from different perspectives. As illustrated, neat EP presented a badly fragmentary state and almost burned out. However, with the incorporation of PCTP, a series of residual chars with a larger size and an increased thickness could be observed. The char layers became more compact, with higher coherence and integrality for EP@PCTP-6 and EP@PCTP-8. The phenomenon was attributed to the catalytic charring effect and intumescent effect of PCTP, which could in turn slow down the heat flux and suppress the fire propagation.

SEM images of the external char residues (**Fig. 8a-d)** show that pure EP presented a discontinuous appearance along with numerous cracks and open holes on the surface, which was beneficial for the emission of combustible volatiles from the inside of the substrate and the exposure of EP matrix to the heat flow outside, thus causing the higher HRR and TSP values. On the contrary, it was apparent that the external char surface got smoother and denser after the addition of PCTP. Interestingly, plenty of unbroken and intumescent bubbles could be captured from the char surface of EP@PCTP-8, which signified the enhanced thermal resistance of the char layer [22]. For the inner structure of the char residues (**Fig. 8e-h**), a similar change was found. Destructive cracks existed in the interior char residue of pure EP, which would promote the heat-

and oxygen-exchanges inside the EP substrate. On the contrary, with the incorporation of PCTP into the EP matrix, the holes and cracks became smaller, more continuous and intumescent surfaces appeared in the interior char residues. The char layers with better integrity and enhanced thermal stability thereby could play as an effective shield to prevent the further pyrolysis of the underlying substrate, to delay the heat and mass transfer, and meanwhile to isolate the oxygen needed in combustion [69, 70].

The vibrations of disordered carbon (D-band) and sp^2-hybridized carbon or graphitic carbon (G-band) can be detected at around 1365 and 1600 cm^{-1}, respectively, in the LRS spectra (**Fig. 8i-l**). Generally, the intensity proportion of the D and G bands (I_D/I_G) reflects the graphitization degree of char, a lower value reveals a higher graphitization degree and a better shield effect [71, 72]. Apparently, pure EP presented the highest I_D/I_G value (2.83), whereas the corresponding I_D/I_G values of EP@PCTP composites reduced with the introducing of PCTP. The EP@PCTP-8 sample showed the lowest I_D/I_G value (2.41) among all the samples, indicating the formation of the char residue with the highest graphitization degree and the most stable property, which was in accordance with the conclusion from the SEM image.

The chemical components of the char residues were further examined by EDS and FTIR experiments to investigate the charring behavior of PCTP. According to the EDS result in **Fig. 8m**, the phosphorus content in the char layer of EP@PCTP-8 was 16.28 wt%, while the nitrogen content was 5.28 wt%. The decreased mass ratio of N/P (from 4.39 to 0.32) for EP@PCTP-8 suggested that the nitrogenous groups such as triazine units in the composite were decomposed and transformed into the gaseous products while burning. In the corresponding FTIR spectrum (**Fig. 8n**), the broad peak detected at 3431 cm^{-1} was derived from the stretching vibrations of O-H and N-H bonds, which came from the phosphoric or polyphosphoric acid, amino compounds or water [73]. The peaks at 1150 and 866 cm^{-1} could be ascribed to the stretching vibrations of P=N and P–N groups in the phosphazene structure. The absorptions around 960 and 1121 cm^{-1} were assigned to the vibrations of P-O-P and P-O-C_{Ar} bonds, indicating the existence of the crosslinked phosphorous oxides in the char layers [74-76]. These results confirmed the catalytic effect and char-forming ability of PCTP during the combustion and revealed its flame-retardant mechanism in condensed phase. However, the triazine groups could not be observed in the FTIR spectrum, it

was possible that the triazine units degraded at high temperature and produced nitrogenous nonflammable gases such as N_2 or NO_2 in the combustion process [39, 77-79], thus functioned with dilution effect in gaseous phase.

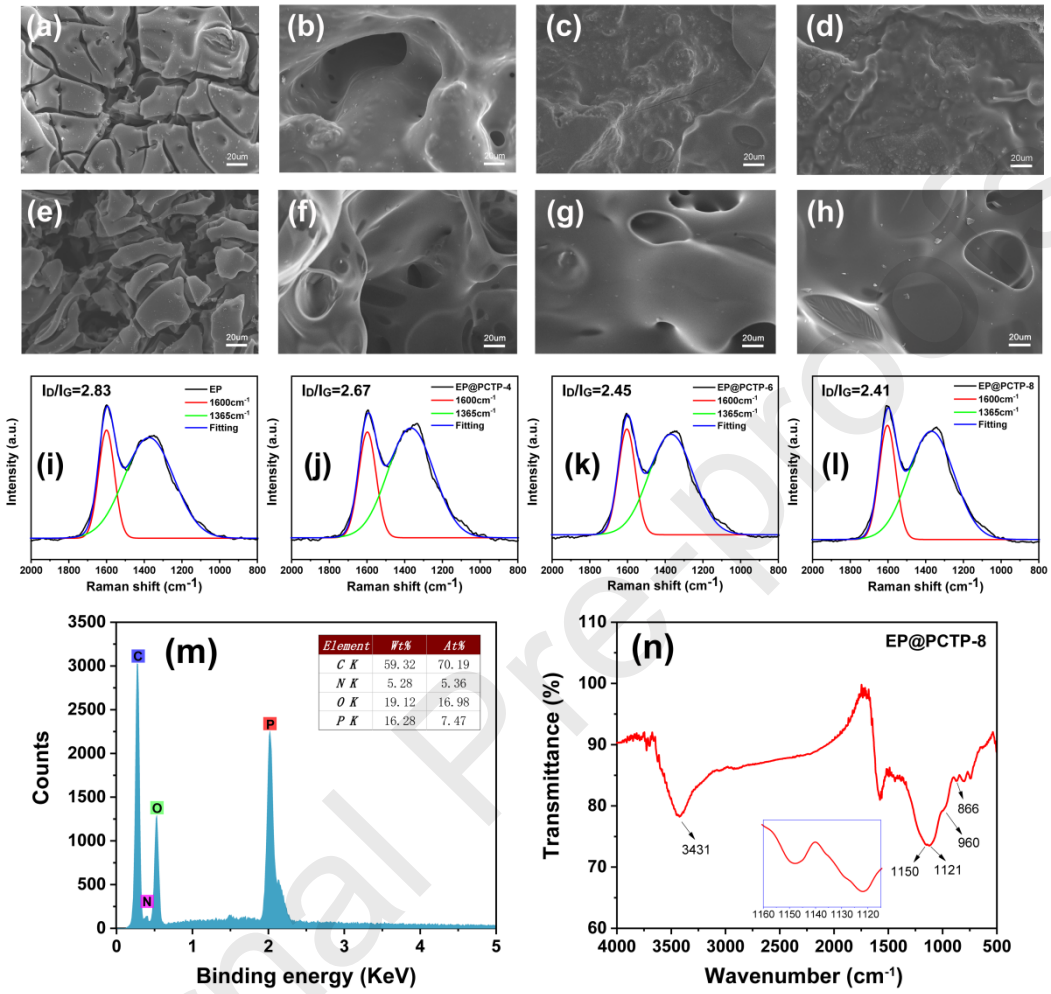

Fig. 8. SEM images of the external char residues of (a) EP, (b) EP@PCTP-4, (c) EP@PCTP-6, (d) EP@PCTP-8; and interior char residues of (e) EP, (f) EP@PCTP-4, (g) EP@PCTP-6, (h) EP@PCTP-8 ; Raman spectra of the char residues of (i) EP, (j) EP@PCTP-4, (k) EP@PCTP-6, (l) EP@PCTP-8; (m) EDS and (n) FTIR spectra of the char residues of EP@PCTP-8.

3.5.2 Evolved gases analysis

The development and spread of the blaze can be significantly influenced by the gasified pyrolysis volatiles generated during the combustion process. Therefore, the thermal pyrolysis behaviors of EP and EP@PCTP composites were analyzed through TG-FTIR technique to further find out the flame retardant mechanism of PCTP in gaseous phase. **Fig. S4** presents the 3D TG-FTIR and FTIR spectra of volatile products from pure EP and EP@PCTP-8 obtained at the

maximum degradation rate. Generally, the FTIR signals of some typical pyrolysis volatiles could be clearly detected at wavenumbers of 3500-3850, 2750-3200, 2250-2400, 1700-1900, 1200-1600 and 600-1000 cm^{-1}. Significant diminutions in pronounced peaks of toxic gaseous volatiles could be easily observed between pure EP and EP@PCTP-8. **Fig. 9a** and **9b** depict the FTIR spectra of the volatile products for EP and EP@PCTP-8 at different temperatures. Signals from primary pyrolysis volatiles located at 3650, 2970, 2360 and 2190, 1740, 1510 and 1260 cm^{-1} in the spectra were assigned to the absorption of -OH (H_2O or phenol), hydrocarbons, CO_2 and CO, carbonyl compounds, aromatic compounds containing aromatic rings or aromatic ethers, respectively [80]. It seemed that the FTIR spectra of EP@PCTP-8 were analogous to that of pure EP. However, the volatile products of EP@PCTP-8 turned up slightly earlier than that of pure EP during the pyrolysis process, indicating the catalytic effect of PCTP in the EP matrix.

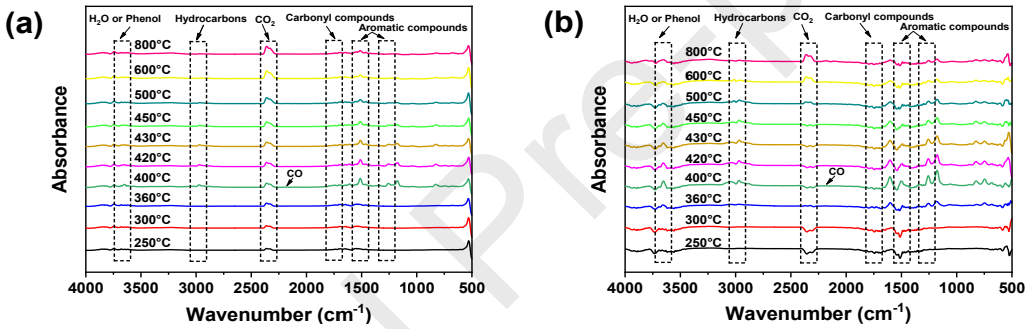

Fig. 9. FTIR spectra of the volatile products for (a) EP and (b) EP@PCTP-8 at different temperatures.

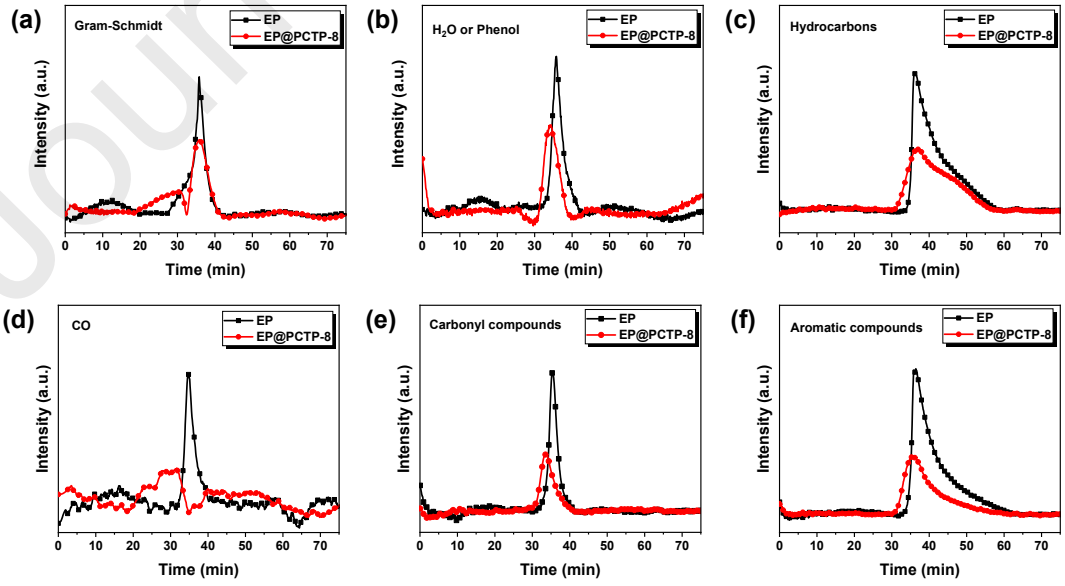

Fig. 10. Absorbance curves of several typical volatile products against time of EP and EP@PCTP-8.

In order to further elucidate the effect of PCTP on the amount of gasified pyrolysis volatiles released during the heating program, the intensities of primary volatile products mentioned above versus time for EP and EP@PCTP-8 are given in **Fig. 10**. It was apparent in **Fig. 10a** that the total volatile products were reduced with the incorporation of PCTP. In addition, the maximum absorbance intensities for EP@PCTP-8 were significantly weaken compared with those of pure EP with respect to volatiles such as H_2O/Phenol, hydrocarbons, CO, carbonyl compounds and aromatic compounds (**Fig. 10b-f**). It is generally accepted that hydrocarbons and aromatic compounds are flammable volatiles, thus the decrease of these volatile products generated would be propitious to the suppression of smoke and heat release during the combustion. Moreover, the intensity of CO diminished greatly, indicating the effect of PCTP on gaseous toxicity suppression, which was coincided with the result of cone calorimeter test.

3.5.3 Proposed flame retardant mechanism

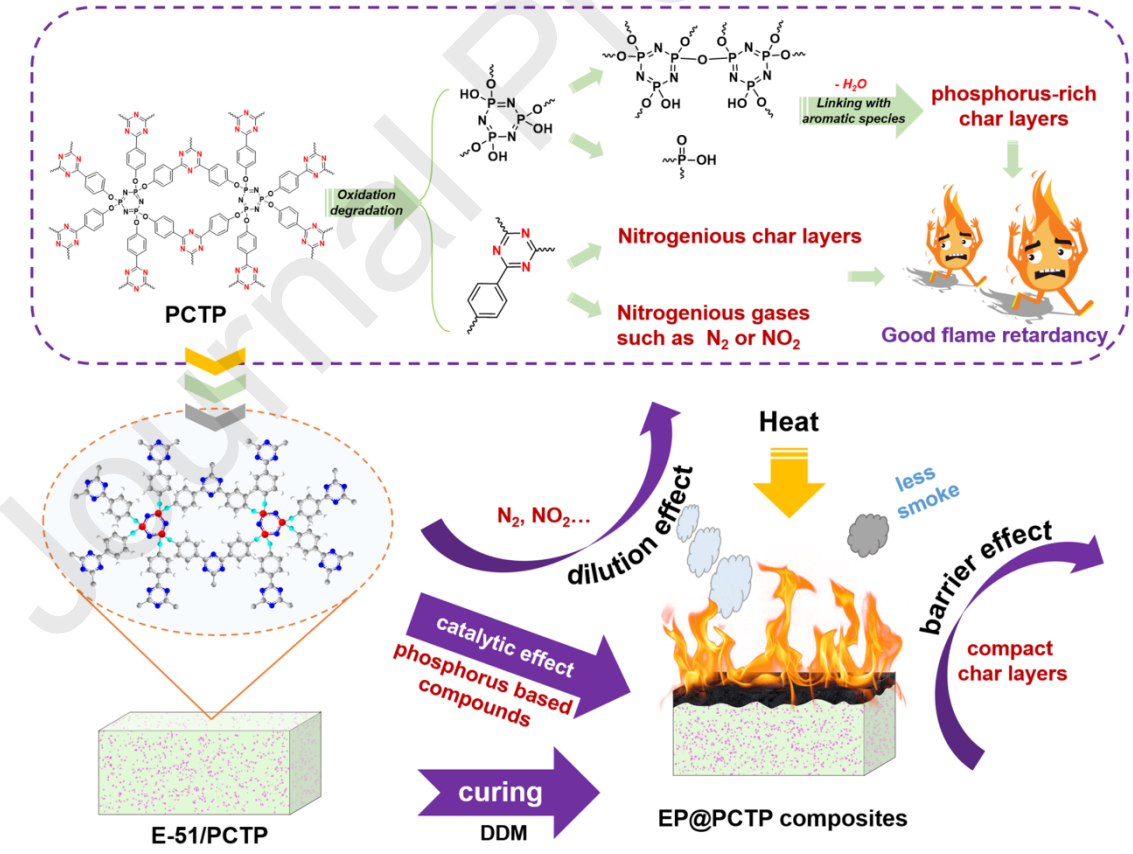

Scheme 2. Schematic illustration of the possible chemical structure evolution and flame retardant

mechanism for PCTP in the EP matrix.

Based on the analysis above, the possible chemical structure evolution and flame retardant mechanism for PCTP in the EP matrix were proposed and illustrated in **Scheme 2**. As a triazine polymer with phosphazene units embedded, PCTP functioned both in condensed and gaseous phases. On the one hand, PCTP could produce phosphorus based compounds such as phosphoric or polyphosphoric acid and crosslinked phosphorous oxides, which work together with the nitrogenous carbon generated during the combustion to promote the formation of the compact and integral char layers, which could in turn cut off the heat flux and oxygen in the air, thus suppressed the fire propagation of EP matrix. In addition, due to the barrier effect of the char layers, the diffusion of pyrolysis volatiles was delayed and led to the decreased smoke release. On the other hand, the nitrogenous nonflammable gases such as N_2 or NO_2 originated from the triazine groups in PCTP could also work in gaseous phase, the dilution effect further contributed to the reduced fire hazard of EP matrix.

3.6 Moisture resistance

Some FRs are moisture sensitive due to their inherent hydrophilicity, which could limit their applications in electronic fields [40, 81]. **Table 5** indicates that the WAP increased over time for all samples. However, EP@PCTP composites showed suppressed WAP, and the water absorption decreased with the increase of PCTP, demonstrating that PCTP could improve the moisture resistance of EP matrix effectively, which might be resulted from the hyper-crosslinked structure and the triazine units in the skeleton of PCTP [82].

3.7 Mechanical properties of EP@PCTP composites

The influence of a flame retardant on the mechanical properties of cured EP materials is a vital factor to evaluate its practical application performance. **Table 5** summarizes the data of EP and EP@PCTP composites after tensile and flexural tests. It can be seen that PCTP had little influence on the tensile strength and flexural strength of EP@PCTP composites, indicating the good compatibilities of PCTP in the EP matrix. In addition, the tensile modulus and flexural modulus increased with the incorporation of PCTP, which could be ascribed to the presence of rigid structures in PCTP. **Fig. S5** shows the SEM images of the tensile fractured surfaces of EP and EP@PCTP composites. It was notable that the fractured surface of pure EP presented a fairly

smooth morphology (**Fig. S5a**), while the surfaces of EP@PCTP composites were quite rough and small crinkles could be observed (**Fig. S5b-d**), which implied the strong interfacial interaction between PCTP and EP matrix. Moreover, the EDS-mappings of P and N elements on the fractured surface of EP@PCTP-8 (**Fig. S5e**, **S5f**) indicated that PCTP had been dispersed uniformly in the EP matrix.

Table 5 Water absorption and mechanical properties of EP and EP@PCTP composites.

Sample	WAP at 70 °C (%)			Tensile strength	Elongation at break	Tensile modulus	Flexural strength	Flexural modulus
	12 h	24 h	48 h	(MPa)	(%)	(GPa)	(MPa)	(GPa)
EP	0.23	0.32	0.65	63.7±2.4	11.2±2.0	1.07±0.05	115.1±7.8	3.55±0.19
EP@PCTP-4	0.14	0.27	0.60	70.9±1.5	8.8±0.3	1.10±0.09	119.8±3.7	3.61±0.20
EP@PCTP-6	0.11	0.19	0.53	68.6±1.2	8.5±0.2	1.15±0.03	121.0±4.2	3.77±0.23
EP@PCTP-8	0.08	0.15	0.47	64.3±1.7	7.8±0.2	1.18±0.04	114.6±1.2	3.90±0.10

4. Conclusions

In this work, a novel polyphosphazene covalent triazine polymer, PCTP, was successfully synthesized through the trimerization reaction of aromatic nitriles substituted HCCP. The phosphorus/nitrogen based PCTP endowed EP thermosets excellent flame retardancy and smoke suppression property. The TGA analysis indicated that EP composites with different PCTP content exhibited an increased thermal resistance and charring property compared with the pure EP. The compact char residues generated could play as a barrier to prohibit the heat and mass transfers and cut off the oxygen supply in the air during the combustion, thus contributed to a large decrease in P-HRR, THR and TSP values. Meanwhile, the triazine units could also decompose into nonflammable volatiles to dilute the ignitable gases during the burning. The LOI values increased dramatically from 22.3% to 28.0% when the content of PCTP moved from 0 to 8.7 phr. The EP composites passed the UL-94 V-0 rating when 6.4 phr PCTP was added. Moreover, the incorporation of PCTP decreased the water absorption, and also brought good compatibility and strong interfacial interaction to EP matrix, thus the T_g values and mechanical properties of EP@PCTP composites were barely influenced, demonstrating its potential practical applications.

5. Declarations of interest

None.

Acknowledgment

The authors acknowledge the financial support from Shanghai Brightfield Chemicals Co. Ltd., China. The authors wish to thank Associate Prof. Dr. Yun Ding and Prof. Dr. Aiguo Hu for their kindly assistance.

References

[1] F.L. Jin, X. Li, S.J. Park, Synthesis and application of epoxy resins: A review, J. Ind. Eng. Chem. 29 (2015) 1-11.

[2] H. Gu, J. Guo, H. Wei, S. Guo, J. Liu, Y. Huang, M.A. Khan, X. Wang, D.P. Young, S. Wei, Z. Guo, Strengthened Magnetoresistive Epoxy Nanocomposite Papers Derived from Synergistic Nanomagnetite-Carbon Nanofiber Nanohybrids, Adv. Mater. 27 (2015) 6277-6282.

[3] R. Auvergne, S. Caillol, G. David, B. Boutevin, J.P. Pascault, Biobased thermosetting epoxy: present and future, Chem. Rev. 114 (2014) 1082-1115.

[4] Y. Qiu, L.J. Qian, H.S. Feng, S.L. Jin, J.W. Hao, Toughening Effect and Flame-Retardant Behaviors of Phosphaphenanthrene/Phenylsiloxane Bigroup Macromolecules in Epoxy Thermoset, Macromolecules 51 (2018) 9992-10002.

[5] Y.J. Xu, J. Wang, Y. Tan, M. Qi, L. Chen, Y.Z. Wang, A novel and feasible approach for one-pack flame-retardant epoxy resin with long pot life and fast curing, Chem. Eng. J. 337 (2018) 30-39.

[6] E.N. Kalali, X. Wang, D.-Y. Wang, Functionalized layered double hydroxide-based epoxy nanocomposites with improved flame retardancy and mechanical properties, J. Mater. Chem. A 3 (2015) 6819-6826.

[7] W. Xu, X. Wang, Y. Wu, W. Li, C. Chen, Functionalized graphene with Co-ZIF adsorbed borate ions as an effective flame retardant and smoke suppression agent for epoxy resin, J. Hazard. Mater. 363 (2019) 138-151.

[8] B. Yu, W. Xing, W. Guo, S. Qiu, X. Wang, S. Lo, Y. Hu, Thermal exfoliation of hexagonal boron nitride for effective enhancements on thermal stability, flame retardancy and smoke suppression of epoxy resin nanocomposites via sol-gel process, J. Mater. Chem. A 4 (2016)

7330-7340.

[9] M.P. Luda, A.I. Balabanovich, M. Zanetti, Pyrolysis of fire retardant anhydride-cured epoxy resins, J. Anal. Appl. Pyrolysis 88 (2010) 39-52.

[10] H.C. Chang, H.T. Lin, C.H. Lin, W.C. Su, Facile preparation of a phosphinated bisphenol and its low water-absorption epoxy resins for halogen-free copper clad laminates, Polym. Degrad. Stab. 98 (2013) 102-108.

[11] X. Wang, Y. Hu, L. Song, W.Y. Xing, H.D.A. Lu, P. Lv, G.X. Jie, Flame retardancy and thermal degradation mechanism of epoxy resin composites based on a DOPO substituted organophosphorus oligomer, Polymer 51 (2010) 2435-2445.

[12] C.H. Lin, Y.C. Chou, W.F. Shiao, M.W. Wang, High temperature, flame-retardant, and transparent epoxy thermosets prepared from an acetovanillone-based hydroxyl poly(ether sulfone) and commercial epoxy resins, Polymer 97 (2016) 300-308.

[13] X.-F. Liu, B.-W. Liu, X. Luo, D.-M. Guo, H.-Y. Zhong, L. Chen, Y.-Z. Wang, A novel phosphorus-containing semi-aromatic polyester toward flame retardancy and enhanced mechanical properties of epoxy resin, Chem. Eng. J. 380 (2020) 122471.

[14] J. Alongi, Z.D. Han, S. Bourbigot, Intumescence: Tradition versus novelty. A comprehensive review, Prog. Polym. Sci. 51 (2015) 28-73.

[15] C. Wentrup, Flash Vacuum Pyrolysis of Azides, Triazoles, and Tetrazoles, Chem. Rev. 117 (2017) 4562-4623.

[16] P. Wang, Z.S. Cai, Highly efficient flame-retardant epoxy resin with a novel DOPO-based triazole compound: Thermal stability, flame retardancy and mechanism, Polym. Degrad. Stab. 137 (2017) 138-150.

[17] I. van der Veen, J. de Boer, Phosphorus flame retardants: Properties, production, environmental occurrence, toxicity and analysis, Chemosphere 88 (2012) 1119-1153.

[18] S. Huo, J. Wang, S. Yang, J. Wang, B. Zhang, B. Zhang, X. Chen, Y. Tang, Synthesis of a novel phosphorus-nitrogen type flame retardant composed of maleimide, triazine-trione, and phosphaphenanthrene and its flame retardant effect on epoxy resin, Polym. Degrad. Stab. 131 (2016) 106-113.

[19] Z.B. Shao, M.X. Zhang, Y. Li, Y. Han, L. Ren, C. Deng, A novel multi-functional polymeric

curing agent: Synthesis, characterization, and its epoxy resin with simultaneous excellent flame retardance and transparency, Chem. Eng. J. 345 (2018) 471-482.

[20] P.J. Wang, D.J. Liao, X.P. Hu, N. Pan, W.X. Li, D.Y. Wang, Y. Yao, Facile fabrication of biobased P-N-C-containing nano-layered hybrid: Preparation, growth mechanism and its efficient fire retardancy in epoxy, Polym. Degrad. Stab. 159 (2019) 153-162.

[21] S. Gaan, G. Sun, K. Hutches, M.H. Engelhard, Effect of nitrogen additives on flame retardant action of tributyl phosphate: Phosphorus–nitrogen synergism, Polym. Degrad. Stab. 93 (2008) 99-108.

[22] H. Duan, Y. Chen, S. Ji, R. Hu, H. Ma, A novel phosphorus/nitrogen-containing polycarboxylic acid endowing epoxy resin with excellent flame retardance and mechanical properties, Chem. Eng. J. 375 (2019) 121916.

[23] X. Hu, H. Yang, Y. Jiang, H. He, H. Liu, H. Huang, C. Wan, Facile synthesis of a novel transparent hyperbranched phosphorous/nitrogen-containing flame retardant and its application in reducing the fire hazard of epoxy resin, J. Hazard. Mater. 379 (2019) 120793.

[24] M. Gleria, R. De Jaeger, Aspects of Phosphazene Research, J. Inorg. Organomet. Polym. 11 (2001) 1-45.

[25] H. Henke, O. Bruggemann, I. Teasdale, Branched Macromolecular Architectures for Degradable, Multifunctional Phosphorus-Based Polymers, Macromol. Rapid Commun. 38 (2017) 1600644.

[26] Q.C. Pan, Phosphazene compound comprising cyano group, preparation method and uses thereof, in: Patent U. S 20170197998 A1, 2017.

[27] L. Wang, Y.X. Yang, X.Y. Shi, S. Mignani, A.M. Caminade, J.P. Majoral, Cyclotriphosphazene core-based dendrimers for biomedical applications: an update on recent advances, J. Mater. Chem. B 6 (2018) 884-895.

[28] S. Rothemund, I. Teasdale, Preparation of polyphosphazenes: a tutorial review, Chem. Soc. Rev. 45 (2016) 5200-5215.

[29] Z.K. Li, G.H. Wang, C. Liang, A.Q. Zhang, Synthesis of cyclotriphosphazene-containing polymeric nanotubes and their use as metal-free photocatalysts for methylene blue degradation, Appl. Surf. Sci. 347 (2015) 541-547.

[30] J. Sun, Z. Yu, X. Wang, D. Wu, Synthesis and Performance of Cyclomatrix Polyphosphazene Derived from Trispiro-Cyclotriphosphazene as a Halogen-Free Nonflammable Material, Acs Sustain. Chem. Eng. 2 (2013) 231-238.

[31] H. Liu, X.D. Wang, D.Z. Wu, Synthesis of a novel linear polyphosphazene-based epoxy resin and its application in halogen-free flame-resistant thermosetting systems, Polym. Degrad. Stab. 118 (2015) 45-58.

[32] S. Yang, J. Wang, S.Q. Huo, J.P. Wang, Y.S. Tang, Synthesis of a phosphorus/nitrogen-containing compound based on maleimide and cyclotriphosphazene and its flame-retardant mechanism on epoxy resin, Polym. Degrad. Stab. 126 (2016) 9-16.

[33] Y.J. Chen, W. Wang, Y. Qiu, L.S. Li, L.J. Qian, F. Xin, Terminal group effects of phosphazene-triazine bi-group flame retardant additives in flame retardant polylactic acid composites, Polym. Degrad. Stab. 140 (2017) 166-175.

[34] P.Y. Wen, Q.L. Tai, Y. Hu, R.K.K. Yuen, Cyclotriphosphazene-Based Intumescent Flame Retardant against the Combustible Polypropylene, Ind. Eng. Chem. Res. 55 (2016) 8018-8024.

[35] J. Artz, Covalent Triazine-based Frameworks-Tailor-made Catalysts and Catalyst Supports for Molecular and Nanoparticulate Species, ChemCatChem 10 (2018) 1753-1771.

[36] P. Kuhn, M. Antonietti, A. Thomas, Porous, covalent triazine-based frameworks prepared by ionothermal synthesis, Angew. Chem. Int. Ed. Engl. 47 (2008) 3450-3453.

[37] S. Ren, M.J. Bojdys, R. Dawson, A. Laybourn, Y.Z. Khimyak, D.J. Adams, A.I. Cooper, Porous, fluorescent, covalent triazine-based frameworks via room-temperature and microwave-assisted synthesis, Adv. Mater. 24 (2012) 2357-2361.

[38] Y. Wang, M.-J. Xu, B. Li, Synthesis of N-methyl triazine-ethylenediamine copolymer charring foaming agent and its enhancement on flame retardancy and water resistance for polypropylene composites, Polym. Degrad. Stab. 131 (2016) 20-29.

[39] P.Y. Wen, X.F. Wang, B.B. Wang, B.H. Yuan, K.Q. Zhou, L. Song, Y.A. Hu, R.K.K. Yuen, One-pot synthesis of a novel s-triazine-based hyperbranched charring foaming agent and its enhancement on flame retardancy and water resistance of polypropylene, Polym. Degrad. Stab. 110 (2014) 165-174.

[40] L.B. Liu, Y. Xu, M.J. Xu, Z.Q. Li, Y.M. Hu, B. Li, Economical and facile synthesis of a highly efficient flame retardant for simultaneous improvement of fire retardancy, smoke suppression and moisture resistance of epoxy resins, Compos Part B-Eng 167 (2019) 422-433.

[41] G.A. Carriedo, L. Fernández-Catuxo, F.J.G. Alonso, P.G. Elipe, P.A. González, G. Sánchez, On the synthesis of functionalized cyclic and polymeric aryloxyphosphazenes from phenols, J. Appl. Polym. Sci. 60 (1996) 2307-2307.

[42] S. Qiu, Y. Shi, B. Wang, X. Zhou, J. Wang, C. Wang, C.S.R. Gangireddy, R.K.K. Yuen, Y. Hu, Constructing 3D Polyphosphazene Nanotube@Mesoporous Silica@Bimetallic Phosphide Ternary Nanostructures via Layer-by-Layer Method: Synthesis and Applications, ACS Appl. Mater. Interfaces 9 (2017) 23027-23038.

[43] N. Amarnath, D. Appavoo, B. Lochab, Eco-Friendly Halogen-Free Flame Retardant Cardanol Polyphosphazene Polybenzoxazine Networks, Acs Sustain. Chem. Eng. 6 (2017) 389-402.

[44] X. Zhu, C. Tian, S.M. Mahurin, S.H. Chai, C. Wang, S. Brown, G.M. Veith, H. Luo, H. Liu, S. Dai, A superacid-catalyzed synthesis of porous membranes based on triazine frameworks for CO_2 separation, J. Am. Chem. Soc. 134 (2012) 10478-10484.

[45] Y. Fu, Z. Wang, S. Li, X. He, C. Pan, J. Yan, G. Yu, Functionalized Covalent Triazine Frameworks for Effective CO_2 and SO_2 Removal, ACS Appl. Mater. Interfaces 10 (2018) 36002-36009.

[46] P. Rekha, V. Sharma, P. Mohanty, Synthesis of cyclophosphazene bridged mesoporous organosilicas for CO_2 capture and Cr (VI) removal, Microporous Mesoporous Mater. 219 (2016) 93-102.

[47] R. Muhammad, P. Rekha, P. Mohanty, Aminal linked inorganic–organic hybrid nanoporous materials (HNMs) for CO_2 capture and H_2 storage applications, RSC Adv. 6 (2016) 17100-17105.

[48] J. Liu, W. Zan, K. Li, Y. Yang, F. Bu, Y. Xu, Solution Synthesis of Semiconducting Two-Dimensional Polymer via Trimerization of Carbonitrile, J. Am. Chem. Soc. 139 (2017) 11666-11669.

[49] Y.Z. Zhu, M. Qiao, W.C. Peng, Y. Li, G.L. Zhang, F.B. Zhang, Y.F. Li, X.B. Fan, Rapid

exfoliation of layered covalent triazine-based frameworks into N-doped quantum dots for the selective detection of Hg^{2+} ions, J. Mater. Chem. A 5 (2017) 9272-9278.

[50] O. Buyukcakir, R. Yuksel, Y. Jiang, S.H. Lee, W.K. Seong, X. Chen, R.S. Ruoff, Synthesis of Porous Covalent Quinazoline Networks (CQNs) and Their Gas Sorption Properties, Angew. Chem. Int. Ed. Engl. 58 (2019) 872-876.

[51] G. Yang, W.H. Wu, Y.H. Wang, Y.H. Jiao, L.Y. Lu, H.Q. Qu, X.Y. Qin, Synthesis of a novel phosphazene-based flame retardant with active amine groups and its application in reducing the fire hazard of Epoxy Resin, J. Hazard. Mater. 366 (2019) 78-87.

[52] Y.J. Zhou, L.X. Zhang, J.J. Liu, X.Q. Fan, B.Z. Wang, M. Wang, W.C. Ren, J. Wang, M.L. Li, J.L. Shi, Brand new P-doped g-C_3N_4: enhanced photocatalytic activity for H-2 evolution and Rhodamine B degradation under visible light, J. Mater. Chem. A 3 (2015) 3862-3867.

[53] S.L. Qiu, Y.X. Hu, Y.Q. Shi, Y.B. Hou, Y.C. Kan, F.K. Chu, H. Sheng, R.K.K. Yuen, W.Y. Xing, In situ growth of polyphosphazene particles on molybdenum disulfide nanosheets for flame retardant and friction application, Compos Part a-Appl S 114 (2018) 407-417.

[54] Y. Gao, Y.Z. Yu, The synergistic effect of dicyandiamide and resorcinol in the curing of epoxy resins, J. Appl. Polym. Sci. 89 (2003) 1869-1874.

[55] G.Y. Wang, Z.B. Nie, Synthesis of a novel phosphorus-containing epoxy curing agent and the thermal, mechanical and flame-retardant properties of the cured products, Polym. Degrad. Stab. 130 (2016) 143-154.

[56] G.R. Xu, M.J. Xu, B. Li, Synthesis and characterization of a novel epoxy resin based on cyclotriphosphazene and its thermal degradation and flammability performance, Polym. Degrad. Stab. 109 (2014) 240-248.

[57] K. Zhou, J. Liu, Y. Shi, S. Jiang, D. Wang, Y. Hu, Z. Gui, MoS_2 nanolayers grown on carbon nanotubes: an advanced reinforcement for epoxy composites, ACS Appl. Mater. Interfaces 7 (2015) 6070-6081.

[58] Y.J. Xu, L. Chen, W.H. Rao, M. Qi, D.M. Guo, W. Liao, Y.Z. Wang, Latent curing epoxy system with excellent thermal stability, flame retardance and dielectric property, Chem. Eng. J. 347 (2018) 223-232.

[59] J. Zhang, X. Mi, S. Chen, Z. Xu, D. Zhang, M. Miao, J. Wang, A bio-based hyperbranched

flame retardant for epoxy resins, Chem. Eng. J. 381 (2020).

[60] Y.Q. Shi, T. Fu, Y.J. Xu, D.F. Li, X.L. Wang, Y.Z. Wang, Novel phosphorus-containing halogen-free ionic liquid toward fire safety epoxy resin with well-balanced comprehensive performance, Chem. Eng. J. 354 (2018) 208-219.

[61] P. Wang, L. Chen, H. Xiao, Flame retardant effect and mechanism of a novel DOPO based tetrazole derivative on epoxy resin, J. Anal. Appl. Pyrolysis 139 (2019) 104-113.

[62] R.K. Jian, Y.F. Ai, L. Xia, L.J. Zhao, H.B. Zhao, Single component phosphamide-based intumescent flame retardant with potential reactivity towards low flammability and smoke epoxy resins, J. Hazard. Mater. 371 (2019) 529-539.

[63] S. Qiu, Y. Zhou, X. Zhou, T. Zhang, C. Wang, R.K.K. Yuen, W. Hu, Y. Hu, Air-Stable Polyphosphazene-Functionalized Few-Layer Black Phosphorene for Flame Retardancy of Epoxy Resins, Small 15 (2019) 1805175.

[64] L.J. Qian, L.J. Ye, G.Z. Xu, J. Liu, J.Q. Guo, The non-halogen flame retardant epoxy resin based on a novel compound with phosphaphenanthrene and cyclotriphosphazene double functional groups, Polym. Degrad. Stab. 96 (2011) 1118-1124.

[65] B. Zhao, W.J. Liang, J.S. Wang, F. Li, Y.Q. Liu, Synthesis of a novel bridged-cyclotriphosphazene flame retardant and its application in epoxy resin, Polym. Degrad. Stab. 133 (2016) 162-173.

[66] W.J. Liang, B. Zhao, P.H. Zhao, C.Y. Zhang, Y.Q. Liu, Bisphenol-S bridged penta(anilino)cyclotriphosphazene and its application in epoxy resins: Synthesis, thermal degradation, and flame retardancy, Polym. Degrad. Stab. 135 (2017) 140-151.

[67] Z. Li, S.I.M. Lira, L. Zhang, D.F. Exposito, V.B. Heeralal, D.Y. Wang, Bio-inspired engineering of boron nitride with iron-derived nanocatalyst toward enhanced fire retardancy of epoxy resin, Polym. Degrad. Stab. 157 (2018) 119-130.

[68] B.H. Yuan, Y.R. Sun, X.F. Chen, Y.Q. Shi, H.M. Dai, S. He, Poorly-/well-dispersed graphene: Abnormal influence on flammability and fire behavior of intumescent flame retardant, Compos Part a-Appl S 109 (2018) 345-354.

[69] J. Liu, J.Y. Tang, X.D. Wang, D.Z. Wu, Synthesis, characterization and curing properties of a novel cyclolinear phosphazene-based epoxy resin for halogen-free flame retardancy and high

performance, RSC Adv. 2 (2012) 5789-5799.

[70] J. Sun, X. Wang, D. Wu, Novel spirocyclic phosphazene-based epoxy resin for halogen-free fire resistance: synthesis, curing behaviors, and flammability characteristics, ACS Appl. Mater. Interfaces 4 (2012) 4047-4061.

[71] A.C. Ferrari, D.M. Basko, Raman spectroscopy as a versatile tool for studying the properties of graphene, Nat. Nanotechnol. 8 (2013) 235-246.

[72] J.N. Wu, L. Chen, T. Fu, H.B. Zhao, D.M. Guo, X.L. Wang, Y.Z. Wang, New application for aromatic Schiff base: High efficient flame-retardant and anti-dripping action for polyesters, Chem. Eng. J. 336 (2018) 622-632.

[73] Y.W. Bai, X.D. Wang, D.Z. Wu, Novel Cyclolinear Cyclotriphosphazene-Linked Epoxy Resin for Halogen-Free Fire Resistance: Synthesis, Characterization, and Flammability Characteristics, Ind. Eng. Chem. Res. 51 (2012) 15064-15074.

[74] H. Liu, X.D. Wang, D.Z. Wu, Novel cyclotriphosphazene-based epoxy compound and its application in halogen-free epoxy thermosetting systems: Synthesis, curing behaviors, and flame retardancy, Polym. Degrad. Stab. 103 (2014) 96-112.

[75] H. Liu, X.D. Wang, D.Z. Wu, Preparation, isothermal kinetics, and performance of a novel epoxy thermosetting system based on phosphazene-cyclomatrix network for halogen-free flame retardancy and high thermal stability, Thermochim. Acta 607 (2015) 60-73.

[76] T. Zhang, Q. Cai, D.Z. Wu, R.G. Jin, Phosphazene cyclomatrix network polymers: Some aspects of the synthesis, characterization, and flame-retardant mechanisms of polymer, J. Appl. Polym. Sci. 95 (2005) 880-889.

[77] X. Zhang, L. Liu, Y. Yu, L. Weng, Flame-Retardant Mechanism of Benzoxazine Resin with Triazine Structure, Adv. Polym. Tech. 37 (2018) 384-389.

[78] A. Bhunia, V. Vasylyeva, C. Janiak, From a supramolecular tetranitrile to a porous covalent triazine-based framework with high gas uptake capacities, Chem Commun (Camb) 49 (2013) 3961-3963.

[79] L. Hao, S. Zhang, R. Liu, J. Ning, G. Zhang, L. Zhi, Bottom-up construction of triazine-based frameworks as metal-free electrocatalysts for oxygen reduction reaction, Adv. Mater. 27 (2015) 3190-3195.

[80] Y. Hou, W. Hu, Z. Gui, Y. Hu, A novel Co(Ⅱ)–based metal-organic framework with phosphorus-containing structure: Build for enhancing fire safety of epoxy, Compos. Sci. Technol. 152 (2017) 231-242.

[81] H. Alamri, I.M. Low, Effect of water absorption on the mechanical properties of nano-filler reinforced epoxy nanocomposites, Mater. Des. 42 (2012) 214-222.

[82] W. Wang, P.Y. Wen, J. Zhan, N.N. Hong, W. Cai, Z. Gui, Y. Hu, Synthesis of a novel charring agent containing pentaerythritol and triazine structure and its intumescent flame retardant performance for polypropylene, Polym. Degrad. Stab. 144 (2017) 454-463.

Highlights

- Polyphosphazene covalent triazine polymer (PCTP) as a flame retardant was synthesized.
- PCTP significantly decreased the fire hazard of epoxy resin (EP).
- PCTP functioned both in condensed and gaseous phases.
- PCTP effectively enhanced the water resistance of EP.
- The T_g values and mechanical properties of EP@PCTP composites were barely influenced.